

**Model of a 80 K Liner Vacuum System for the
4.2 K Cold Bore of the SSCL 20 TeV Proton Collider**

W. Turner

Superconducting Super Collider Laboratory*
2550 Beckleymeade Ave.
Dallas, TX 75237

September 1993

*Operated by the Universities Research Association, Inc., for the U.S. Department of Energy under Contract No. DE-AC35-89ER40486.

MASTER

Se

DISTRIBUTION OF THIS DOCUMENT IS UNLIMITED

Model of a 80 K liner vacuum system for the 4.2 K cold bore of the SSCL 20 TeV proton collider

W. C. Turner

Abstract

In this paper we discuss a model for an 80 K liner system for the beam tube vacuum of the Superconducting Super Collider (SSC). The liner is a coaxial perforated tube fitting inside the ~4.2 K bore tube of the SSC magnet cryostats. A liner of this type is useful for pumping the gas desorbed by synchrotron radiation out of the view of the radiation and for decoupling the beam current from the 4.2 K refrigeration plant capacity. Addition of cryosorber on the bore tube (e.g., charcoal) greatly increases the H₂ sorption capacity compared to the bare metal surface, thus lengthening the time between beam tube warmups. The model equations are useful for estimating the performance of the beam tube vacuum and for defining the experimental information necessary to make a prediction. Some analysis is also presented for 4.2 K and 20 K liners and a simple 4.2 K beam tube without a liner.

1.0 INTRODUCTION

This report describes a model of a 80 K liner configuration for the beam tube vacuum system for the 87 km SSCL Collider rings. The feature of the Collider which leads to the consideration of a liner is the combination of synchrotron light emitted by the ultra relativistic 20 TeV protons with superconducting magnets. The function of the type of liner described here is twofold; to pump gases photodesorbed by the synchrotron light emitted by ultra relativistic protons and to absorb the synchrotron radiation heat load at a temperature higher than the 4.2 K temperature of the superconducting magnet cryostats. The model described here is to be used for choosing parameters and estimating machine performance. Early considerations of a liner for the SSCL Collider rings are contained in the report by H. Edwards¹ and for the CERN Large Hadron Collider (LHC) in Chapter 7 of the design study for LHC.² The first clear statement of the potential problems that may be encountered by a smooth bore 4.2 K beam tube vacuum system without a liner was given by A. Maschke in Appendix 1 of Reference 1.

A schematic diagram of the liner configuration to be analyzed is given in Figure 1. The liner is a tube located coaxially inside the 4.2 K bore tube of the superconducting magnet cryostats. The liner shown in Figure 1 is maintained at 80 K by the flow of high pressure GHe in tubes brazed to the outside wall of the liner. Low thermal conductivity supports hold the liner in position. Holes in the liner allow photodesorbed gases to pass from the inside of the liner to the outside where it is cryosorbed on either the 4.2 K bore tube surface or the cryosorber that has been bonded to the bore tube surface. The inside surface of the liner is chosen to be Cu to avoid excessive parasitic heating by beam image currents and to have resistive wall instability growth time long enough for feedback stabilization. However the Cu by itself is not strong enough to withstand the Lorentz forces in a magnet quench so the liner tube has an outer layer of SS tubing. There are many technical details that need to be dealt

with in the design of a practical liner system—heat leaks to the 4.2 K cryostat, differential thermal expansion and contraction, quench survivability, interface with beam position monitors, RF impedance and beam stability and so on. Here we will only deal with the vacuum performance. Some details of the design of a 80 K liner system may be found in the paper of Shu *et al.*³

From the vacuum viewpoint the purpose of the liner is to increase the pumping capacity for hydrogen and to reduce the accumulation of weakly bound photodesorbed gases on the surface of the beam tube that is directly exposed to synchrotron radiation. The operational gain is a reduction in the number of beam tube warm ups that are required in order to operate with acceptable beam current and luminosity. Hydrogen is a particular problem because of its relatively high isotherm pressure at 4.2 K, which precludes the accumulation of even one monolayer due to the excessive heat deposited in the magnet cryostats by nuclear scattering on gas molecules. As Maschke has pointed out,⁴ this is a local problem, the entire vacuum system availability is characterized by photodesorption from the least conditioned part of the system—*e.g.*, the components most recently vented to atmosphere or installed—and not by an average over the entire circumference of the Collider rings. Once the hydrogen pumping problem has been dealt with, as in the liner configuration with a cryosorbing material, then nuclear and Coulomb scattering of the high energy Collider proton beams are dominated by the photodesorption of heavier gases—primarily CO and CO₂.

At 20 TeV and design beam current 0.072 A in each ring the synchrotron radiation power is 0.140 W/m or 9 kW per ring. The photon flux is 10¹⁶ photons/m/s with critical energy 284 eV. This heat load amounts to about one third of the Collider 4.2 K refrigeration capacity (67.5 kW) and has been included in the baseline Collider configuration without a liner. From the heat load viewpoint the particular liner discussed in this paper is primarily of interest for upgraded operation—say at three times baseline beam current where it would be an alternative to increasing the 4.2 K refrigeration capacity.

Model of a 80 K liner vacuum system for the 4.2 K cold bore of the SSCL 20 TeV proton collider

W. C. Turner

Abstract

In this paper we discuss a model for an 80 K liner system for the beam tube vacuum of the Superconducting Super Collider (SSC). The liner is a coaxial perforated tube fitting inside the ~4.2 K bore tube of the SSC magnet cryostats. A liner of this type is useful for pumping the gas desorbed by synchrotron radiation out of the view of the radiation and for decoupling the beam current from the 4.2 K refrigeration plant capacity. Addition of cryosorber on the bore tube (e.g., charcoal) greatly increases the H₂ sorption capacity compared to the bare metal surface, thus lengthening the time between beam tube warmups. The model equations are useful for estimating the performance of the beam tube vacuum and for defining the experimental information necessary to make a prediction. Some analysis is also presented for 4.2 K and 20 K liners and a simple 4.2 K beam tube without a liner.

The luminosity lifetime goal for the vacuum system is 150 hrs at 20 TeV and 0.072 Å. Assuming the design luminosity $10^{33} \text{ cm}^{-2}\text{s}^{-1}$ is actually reached at 0.072 Å this would ensure that the decrease in luminosity due to collisions at the interaction points (IP's) would dominate the vacuum effect.⁵ From the viewpoint of 150 hrs luminosity lifetime the upper bound on density for each of the molecular species usually observed in photodesorption experiments is $3 \times 10^8 \text{ H}_2/\text{cm}^3$, $6.5 \times 10^7 \text{ CH}_4/\text{cm}^3$, $5 \times 10^7 \text{ CO}/\text{cm}^3$ and $3.3 \times 10^7 \text{ CO}_2/\text{cm}^3$.

The molecular densities given in the previous paragraph are global limits that apply to an average over the entire length of the Collider beam tube. Local upper bounds are determined by the limiting power density ($\sim 0.6 \text{ W/m}$)⁶ that can be deposited in the dipole magnet cryostats by nuclear scattering without overloading the cryogenic system and/or causing a magnet quench. For the various gases the corresponding upper bounds on density are $4 \times 10^{10} \text{ H}_2/\text{cm}^3$, $8.7 \times 10^9 \text{ CH}_4/\text{cm}^3$, $7 \times 10^9 \text{ CO}/\text{cm}^3$ and $4.4 \times 10^9 \text{ CO}_2/\text{cm}^3$. H₂ presents a special case because its saturation isotherm density is $2.0 \times 10^{12} \text{ H}_2/\text{cm}^3$ at 4.2 K.

The liner issues are somewhat different for the SSCL Collider than for the LHC proposed at CERN.² The LHC has 1.8 K magnet cryostats so removing the synchrotron radiation at a temperature higher than the superconducting magnets is the primary concern and a liner has been designed in from the beginning. At 1.8 K the vapor pressure of H₂ is low enough that it can be pumped by cryocondensation on the wall of the magnet bore tube and an additional cryosorber material is not required.

The goal of this report is to derive equations for the density of molecular species inside the liner tube in terms of the magnitude of photodesorption coefficients, the area of holes in the liner and the cryosorber pumping speed. The calculated densities are then used to estimate the nuclear scattering lifetime. The model equations are derived in Section 2, the trade off between liner hole pumping speed and impedance is described in Section 3, input data for the vacuum calculations are in Section 4 and numerical solutions to the vacuum equations are in Section 5. Additional experimental data has become available since this study was initiated

and much work is in progress. The implications of this new information are contained in Section 6. A summary is provided in Section 7.

2.0 MODEL EQUATIONS

2.1 Two region 80 K liner configuration

The equations for a two region model of the liner are given in this section. Conditions are assumed to be uniform in the axial direction. Conductances, volumes, surface areas and photon flux are understood to be per unit axial length of the beam tube. The treatment is first given for H₂, which is the most complicated case because of its higher isotherm density, and the simplifications for the heavier molecules are noted. The molecular density inside the liner is n₁ and outside is n₂. The density outside the liner is further divided into two components; molecules n₁₂ that have collided with the liner and are moving toward the magnet bore tube and molecules n₂₁ that have collided with the bore tube and are moving toward the liner. The molecules are assumed to move with velocity corresponding to the wall temperature of their last collision. The temperature of the liner is T₁ and the magnet bore tube T₂. We assume T₁ >> T₂ and that T₁ is high enough that we may neglect cryosorption on the liner surfaces. The conductance of the liner holes from inside to outside is C₁₂ and outside to inside C₂₁. The conductances are given by:

$$C_{12} = p \langle v_1 \rangle N_h A_h / 4$$

$$C_{21} = p \langle v_2 \rangle N_h A_h / 2$$

where the molecular speeds are $\langle v_{1,2} \rangle = (8kT_{1,2}/\pi m)^{1/2}$, A_h is the area of a hole, p is the transmission probability through a hole and N_h the number of holes per unit length of beam tube. A factor 1/2 instead of the usual 1/4 appears in C₂₁ because it applies to the directed species n₂₁. The ideal pumping speed of the outside surface of the liner is S₁ and of the inside surface of the bore tube is S₂. These are given by:

$$S_1 = 2\pi a_1 \langle v_2 \rangle / 2$$

$$S_2 = 2\pi a_2 \langle v_1 \rangle / 2$$

where a_1 is the radius of the liner and a_2 the radius of the bore tube. Again the factor $1/2$ instead of $1/4$ appears because S_1 and S_2 apply to the directed species n_{21} and n_{12} respectively. The vacuum equations for n_1 and n_{12} may then be written as:

$$V_1 dn_1/dt = \eta * d\Gamma/dt - C_{12} * n_1 + C_{21} * n_{21} \quad (1)$$

$$V_2 dn_{12}/dt = C_{12} * n_1 + S_1 * n_{21} - C_{21} * n_{21} - S_2 * n_{12} \quad (2)$$

where V_1 is the volume inside the liner, V_2 the volume between the liner and bore tube, $d\Gamma/dt$ is the photon flux per unit length incident on the inside surface of the liner and η is the number of molecules desorbed per incident photon. In the Eqs. (1) and (2), $C_{12} * n_1$ and $C_{21} * n_{21}$ account for the leakage of molecules through the holes in the liner. In Eq. (2), $S_1 * n_{21}$ and $S_2 * n_{12}$ account for the conversion of n_{21} into n_{12} due to wall collisions. The vacuum equation for n_{21} is more involved since it must account for cryosorption on both the cryosorber and the 4.2 K SS bore tube surface that is not covered by cryosorber.

The number of molecules per unit length adsorbed on the cryosorber is N_c and on the SS bore tube surface N_w . The sticking coefficients on these surfaces are σ_c and σ_w , the ideal pumping speeds are S_{2w} and S_{2c} with $S_{2w} + S_{2c} = S_2$. The sojourn times are τ_w and τ_c . The vacuum equations for n_{21} , N_w and N_c are then given by:

$$V_2 dn_{21}/dt = -S_1 * n_{21} + (1 - \sigma_w) S_{2w} * n_{12} + (1 - \sigma_c) S_{2c} * n_{12} \quad (3)$$

$$+ N_w / \tau_w + N_c / \tau_c$$

$$dN_w/dt = \sigma_w S_{2w} * n_{12} - N_w / \tau_w \quad (4)$$

$$dN_c/dt = \sigma_c S_{2c} * n_{12} - N_c / \tau_c. \quad (5)$$

We have neglected cryosorption and condensation of molecules on the 80 K surfaces of the liner.

2.2 Approximate solutions for the two region 80 K liner configuration

Solutions are now given for Eqs. (1) to (5). Since we are generally interested in time scales that are very long compared to the transit time of a molecule between wall collisions we simplify Eqs. (1) to (3) with the quasi-static density approximation $dn_1/dt = dn_{12}/dt = dn_{21}/dt = 0$. For the first solution we further assume the SS bore tube surface and the cryosorber are far from equilibrium, $N_w/\tau_w \ll \sigma_w S_{2w} n_{12}$ and $N_c/\tau_c \ll \sigma_c S_{2c} n_{12}$. In this approximation both the SS bore tube and cryosorber act as good pumps and the adsorbed flux far exceeds thermal evaporation. This approximation should be good for H₂ early in time at the beginning of photodesorption and always good for the heavier gases. We then have:

$$\begin{aligned} n_1 &= (\eta * d\Gamma/dt) / C_{12} * [1 + (C_{21}/S_1) * (S_2 / (S_c + S_w) - 1)] \\ &\approx (\eta * d\Gamma/dt) / C_{12} * [1 + (pN_h A_h / 2\pi a_1) * (1/\sigma_w - 1)] \end{aligned} \quad (6)$$

$$n_{12} = (\eta * d\Gamma/dt) / (S_c + S_w) \quad (7)$$

$$n_{21} = [(S_2 - S_c - S_w) / S_1] * n_{12} \quad (8)$$

$$N_w = [S_w / (S_c + S_w)] * \int dt \eta * d\Gamma/dt \quad (9)$$

$$N_c = [S_c / (S_c + S_w)] * \int dt \eta * d\Gamma/dt. \quad (10)$$

For H₂ this solution begins to be invalid when the surface density $s \equiv (N_w + N_c) / 2\pi a_1$ of H₂ approaches s_m and the density of H₂ thermally desorbing from the surface approaches n_{21} . The effective pumping of the surface dN_c/dt then goes to zero and the SS bore tube surface reaches equilibrium. For the second solution we assume the SS surface is in equilibrium $N_w/\tau_w = \sigma_w S_{2w} n_{12}$ and obtain:

$$n_1 = \eta * d\Gamma/dt / C_{12} + (T_2/T_1)^{1/2} * ((S_2 - S_c)/S_1) * (\eta * d\Gamma/dt) / S_c \quad (11)$$

$$n_{12} = (\eta * d\Gamma/dt) / S_c \quad (12)$$

$$n_{21} = ((S_2 - S_c)/S_1) * (\eta * d\Gamma/dt) / S_c \quad (13)$$

$$N_w / \tau_w = \sigma_w S_{2w} * n_{12} \quad (14)$$

$$N_c = \int dt \eta * d\Gamma/dt. \quad (15)$$

This solution simplifies further with the reasonable assumption that the effective cryosorber pumping speed $S_c = \sigma_c S_{2c}$ is much less than the ideal pumping speed of the entire bore tube wall S_2 . Then we have:

$$n_1 = (1/C_{12} + 1/S_c) * \eta * d\Gamma/dt \quad (16)$$

$$\begin{aligned} n_{21} &= (T_1/T_2)^{1/2} * n_{12} \\ &= (T_1/T_2)^{1/2} * (\eta * d\Gamma/dt) / S_c. \end{aligned} \quad (17)$$

Since the SS surface is in equilibrium the surface density $x = s/s_m$ of H_2 is calculated from the BET equation for the normalized density $y = 2n_{21}/n_{sat}$, Reference~7. The BET eq. is described in Section 4.1. The transition between the regions of validity of the two solutions given by Eqs. (6) to (10) and (11) to (17) occurs when the surface densities of H_2 calculated in the two approximations cross over. When the cryosorber itself begins to saturate the assumption $N_c/\tau_c \ll \sigma_c S_{2c} n_{12}$ will no longer be valid and the hydrogen density will rise toward its saturation value, $\sim 2 \times 10^{12} \text{ H}_2/\text{cm}^3$ at 4.2 K. Operationally when this happens the cryosorber will need to be regenerated due to deterioration of the luminosity lifetime ($\tau_L = 150 \text{ hrs}$ at $3 \times 10^8 \text{ H}_2/\text{cm}^3$) or increasing heat load to the magnet cryostats (vacuum instability and quenching of the superconducting magnets set in at about $4 \times 10^{10} \text{ H}_2/\text{cm}^3$). The capacity

of the cryosorber is to be chosen so the time between beam tube warm ups is acceptably long—say once per operational year.

2.3 Single region 4.2 K beam tube configuration without a liner

In order to compare the beam tube vacuum with a liner to the case without a liner we write down the equations for a single region 4.2 K beam tube. There is then only one equation each for volume density n and surface density s :

$$Vdn/dt = \eta d\Gamma/dt + \eta' d\Gamma/dt - \sigma_w S_w * n + N_w/\tau_w \quad (18)$$

$$dN_w/dt = \sigma_w S_w * n - N_w/\tau_w - \eta' d\Gamma/dt. \quad (19)$$

The ideal wall pumping speed is given by $S_w = \langle v \rangle A_w / 4$ where $\langle v \rangle$ is the mean speed of desorbed molecules. Compared to the warm liner case an additional desorption term $\eta' d\Gamma/dt$ has been added to describe the desorption of cryosorbed molecules previously desorbed by the η process. In the case of a warm liner the cryosorbed molecules are hidden from the photons and this term does not appear. The cryosorbed molecules are relatively weakly bound to the surface and may be easily desorbed. For H_2 cryosorbed to a metal surface the sorption energy is in the range of 0.020 eV. At low surface coverage the desorption coefficient is expected to depend linearly on the surface concentration of cryosorbed molecules, $\eta' = \eta_0'(s/s_m)$. An alternative way of writing the thermal desorption term is $N_w/\tau_w = \sigma_w S_w * n_e$ where n_e is the equilibrium vapor density given by the isotherm for surface density s . We are again interested in the quasi-static solution $dn/dt = 0$, which is given by:

$$n = (\eta d\Gamma/dt)/\sigma_w S_w + (\eta' d\Gamma/dt)/\sigma_w S_w + n_e, \quad (20)$$

$$s = (1/A_w) \int \eta d\Gamma. \quad (21)$$

There are three contributions to the density due to primary desorption, desorption of cryosorbed molecules and the isotherm. The first term would be expected to decrease with exposure to photon flux as the source of tightly bound molecules cleans up. The second term would increase with photon flux due to the accumulation of cryosorbed molecules. Furthermore the first term is linear in photon flux or proton beam current whereas the second term is quadratic in beam current and could become much more serious as the beam current in the Collider is increased. The additional desorption coefficient η' does not increase the inventory of desorbed molecules but amounts to a recycling of previously desorbed molecules. The isotherm density n_e is only important for H_2 . The desorbed molecules steadily build up on the beam tube surface. In the case of H_2 this will necessitate a warm up and pump out of the beam tube at the very least when s approaches a monolayer s_m . In addition the desorption of cryosorbed molecules described by η' could well degrade the luminosity lifetime to the point where the beam tube would have to be warmed up well before reaching one monolayer.

In developing Eqs. (18) to (21) we have implicitly assumed that there is no place on the beam tube wall for the desorbed molecules to hide where they are not exposed to photons, either direct or scattered. When there is such a place the treatment is identical to the 4.2 K liner situation described in paragraph 2.5.

Comparing Eq. (16) with Eq. (20) we see that much less information is needed to specify a vacuum system with a 80 K liner than without. If the cryosorber pumping speed is to be chosen so $S_c \gg C_{12}$, calculations are insensitive to the details of the cryosorber. With an 80 K liner present essentially only the desorption coefficient η is needed to calculate the density. Without a liner many more parameters are needed; η , η' , s_w , $\langle v \rangle$ and n_e . With the 80 K liner the mean molecular speed may be assumed to be the wall temperature since the molecules are not absorbed on the liner wall and a molecule undergoes a large number of wall collisions before passing through a hole to the outer region. With a 4.2 K beam tube and no

liner the desorbed molecules may have a mean speed corresponding to a temperature higher than 4.2 K. It seems likely that the molecules desorbed by the η process, and relatively tightly bound, will have a mean speed much higher than 4.2 K whereas molecules desorbed by the η' process may have a speed comparable to 4.2 K. This complication has been ignored in Eq. (21).

The desorption of cryosorbed molecules in Eq. (18) has been written as though it is photon induced. It is also possible that energetic molecules of a few eV energy desorbed by the primary η process could desorb loosely bound molecules, say with a coefficient η'' molecules per incident molecule. In this case the desorption term would be written as $\eta''(\eta d\Gamma/dt)$ with $\eta'' = \eta_0''(s/s_m)$ at low surface coverage. The parametrization is slightly different than with photon induced desorption but would also lead to a contribution to density increasing with Γ or time.

At 4.2 K it is possible to imagine a photon induced source of surface density in addition to the cryosorption of photodesorbed molecules. In that case Eqs. (18) and (19) are replaced by:

$$Vdn/dt = \eta_1 d\Gamma/dt + \eta' d\Gamma/dt - \sigma_w S_w * n + N_w / \tau_w \quad (22)$$

$$dN_w/dt = \eta_2 d\Gamma/dt + \sigma_w S_w * n - N_w / \tau_w - \eta' d\Gamma/dt. \quad (23)$$

A physical model of $\eta_2 d\Gamma/dt$ would be photon induced production of hydrogen followed by surface recombination to H_2 which remains cryosorbed to the surface. At temperatures high enough that cryosorption may be neglected these molecules would show up in the equation for Vdn/dt . The quasi static solution is:

$$n = (\eta_1 d\Gamma/dt) / \sigma_w S_w + (\eta' d\Gamma/dt) / \sigma_w S_w + n_e, \quad (24)$$

$$s = (1/A_w) \int (\eta_1 + \eta_2) d\Gamma. \quad (25)$$

2.4 20 K liner configuration

The primary purpose of this report is to develop a vacuum model for an 80 K liner. However we want to make some comparative statements for liners at other conveniently chosen temperatures where substantial refrigeration and cryogenic capacity is already being planned. For SSCL these temperatures are 20 K, the temperature of the intermediate thermal shield in the magnet cryostats, or 4.2 K, the temperature of the magnet cryostat cold mass. We will discuss the 20 K configuration in this section and 4.2 K in the following section.

The new feature of the 20 K liner compared to 80 K is that we must allow for cryosorption of CH_4 , CO and CO_2 on the surfaces of the liner. H_2 may be treated the same way as at 80 K. For the molecules heavier than H_2 then we have to add an equation for the surface density on the inside of the liner and also allow for the possibility that these cryosorbed molecules may be photodesorbed. The isotherm density of these molecules may be neglected at 20 K. Since for the heavy molecules the pumping speed of the surfaces outside the liner is very high compared to the conductance of holes in the liner it is reasonable to neglect the streaming of molecules back into the liner from the outside region. This significantly simplifies the equations for the heavy molecules and since we are mainly interested in the density inside the liner we may drop the subscripts dealing with the different regions. We then have the following two equations describing the density n and surface density s for each species of heavy molecules inside the liner:

$$Vdn/dt = \eta * d\Gamma/dt + \eta' * d\Gamma/dt - C * n - \sigma_w * S * n \quad (26)$$

$$dN_w/dt = \sigma_w * S * n - \eta' * d\Gamma/dt \quad (27)$$

where C is the hole conductance and S is the ideal pumping speed of the inside surface of the liner. We will again ignore the possible distinction in molecular velocities between molecules

desorbed by the η and η' processes. Assuming a quasi-static approximation for the density $dn/dt \equiv 0$ the solution to these equations is:

$$n = (\eta + \eta')d\Gamma/dt/(C + \sigma_w * S) \quad (28)$$

$$\begin{aligned} S &= (\sigma_w * S / A_w) * \int n dt - (1/A_w) * \int \eta' * d\Gamma \\ &= (1/A_w) * \int \eta * d\Gamma - (C/A_w) * \int n dt. \end{aligned} \quad (29)$$

In the solution for S , conductance through the holes in the liner competes with the adsorption of molecules on the surface of the liner. A new feature of a cryosorbing wall with a liner compared to one without a liner, or indeed with any place for the molecules to be pumped other than the desorbing wall itself, is that the surface density S may also reach a quasi steady state $ds/dt \equiv 0$, where the molecules sticking to the wall are balanced by those leaving due to recycling. This will only occur if the recycling coefficient η' is non zero. In the region where we may approximate η' by $\eta'_0(s/s_m)$ the solution then takes the form:

$$n = (\eta * d\Gamma/dt) / C \quad (30)$$

$$\eta' = (\sigma_w S / C) * \eta. \quad (31)$$

If a linear dependence of η' on S is assumed, $\eta' = \eta'_0(s/s_m)$ then the solution for surface density is:

$$s/s_m = (\sigma_w / \eta'_0) * (S/C) * \eta. \quad (32)$$

The characteristic time constant for S to reach a quasi steady state is $\tau_s = (A_w * s_m) / (\eta'_0 * d\Gamma/dt)$. Eqs. (30) to (31) predict that as η decreases with increasing photon dose Γ , the density n and surface density S will both decrease with time and eventually all the desorbed gas winds up on the outside of the liner, or at least in a place where it cannot be photodesorbed.

2.5 4.2 K liner configuration

If the liner temperature is 4.2 K then we must allow for cryosorption of H₂ and the H₂ isotherm density inside the liner. The situation is similar to the 4.2 K beam tube without a liner discussed in paragraph 2.3 but with a conductance term added. The molecules heavier than H₂ are treated exactly the same as the 20 K liner, with appropriate change of conductances and pumping speed due to temperature. To simplify the equations we again neglect the streaming of molecules back into the liner from outside. Until the 4.2 K metallic surfaces approach a monolayer the error estimated from Eq. (6) is only a few percent. Once these surfaces approach a monolayer the fractional error from Eq. (16) is given by the ratio of hole conductance to cryosorber pumping speed, C₁₂/S_c. One would expect to choose S_c large enough that the hole conductance is the limiting factor for pumping but practical considerations may require C₁₂/S_c as large as a few tens of percent. The equations describing the density and surface density are:

$$Vdn/dt = \eta d\Gamma/dt + \eta' d\Gamma/dt - C*n - \sigma_w S_w * n + N_w/\tau_w \quad (33)$$

$$dN_w/dt = \sigma_w S_w * n - N_w/\tau_w - \eta' d\Gamma/dt. \quad (34)$$

Again assuming a quasi-static approximation for the density dn/dt ≈ 0 the solution to these equations is:

$$n = (\eta + \eta')d\Gamma/dt/(C + \sigma_w * S) + n_e \quad (35)$$

$$\begin{aligned} s &= (\sigma_w * S / A_w) * \int (n - n_e) dt - (1 / A_w) * \int \eta' * d\Gamma \\ &= (1 / A_w) * \int \eta * d\Gamma - (C / A_w) * \int n dt. \end{aligned} \quad (36)$$

For t >> τ_s = (A_w*s_m)/(η' * dΓ/dt) the surface density is also in a quasi steady state and the solution is:

$$n = (\eta * d\Gamma/dt) / C \quad (37)$$

$$\eta' = (\sigma_w S/C) * (\eta - C * n_e / d\Gamma / dt). \quad (38)$$

With $\eta' = \eta'_0(s/s_m)$ the solution for surface density is:

$$s/s_m = (\sigma_w / \eta'_0) * (S/C) * (\eta - C * n_e / d\Gamma / dt). \quad (39)$$

Comparing Eqs. (6), (11), (30) and (37) with 80 K, 20 K and 4.2 K liners we see that to good approximation, when the surface density has reached a quasi steady state, the density is always given by $n = (\eta * d\Gamma / dt) / C$ and remarkably does not depend on the recycling coefficient η' , the isotherm density or the wall sticking coefficient. The solution for a 4.2 K beam tube without a liner given by Eq. (20) depends on all of these parameters as well as η . We are therefore in the situation where it is much easier to specify a satisfactory liner configuration than a beam tube without a liner since much less needs to be known. For the 80 K liner we can be reasonably sure that the mean molecular speed entering into C is just given by the velocity of molecules with $T = 80$ K since there is no sticking and the molecules must make a large number of wall collisions before leaving through a hole. When the molecules stick at 20 K and 4.2 K the mean velocity of molecules exiting the holes may not correspond to the wall temperature. However it is reasonably certain that the wall temperature corresponds to a lower bound velocity and will give a conservative estimate of liner vacuum performance. For the 20 K and 4.2 K cases where there is sticking, it is true that $n = (\eta * d\Gamma / dt) / C$ does not obtain until the surface has reached steady state and there is some uncertainty in the time for this to occur since the characteristic time constant depends on η'_0 . However until the surface has reached a steady state it is effectively pumping so the true density will actually be lower than estimated by $n = (\eta * d\Gamma / dt) / C$. Once again the liner performance will be underestimated, at least until the surface ceases to pump.

3.0 LINER HOLE GEOMETRY

For a given hole geometry the maximum allowable conductance is limited by beam impedance which must be less than the instability threshold by an agreed upon safety margin. For purposes here we will assume the holes are circular and calculate the impedance from the expression for a hole in a thin wall⁸ with the Gluckstern correction for thickness applied.⁹ This prescription is in reasonable agreement with experimental measurements¹⁰ and numerical simulations^{10,11} of hole impedance. If these assumptions are not the ones ultimately chosen it is a simple matter either to repeat these types of calculations or to match the chosen geometry to the numerical values of the pumping speed that are used here.

The conductance of N_h holes/m of diameter d and thickness t may be written as:

$$C = (\pi/16)pN_h d^2 \langle v \rangle. \quad (40)$$

where $\langle v \rangle$ is the mean molecular speed and $p = p(t/d)$ is the Clausing factor or transmission probability through a hole with finite thickness.¹² The transverse impedance of the holes is:

$$Z_{T,h} = (4/3\pi)gZ_0RN_hd^3/D^4. \quad (41)$$

where $Z_0 = 377$ Ohms, D is the liner diameter, $2\pi R$ is the liner circumference (70.6 km) and $g = g(t/d)$ is the Gluckstern correction factor for hole thickness. For the transverse impedance of everything but the holes the results given by W. Chou¹ have been fit with:

$$Z_{T,t} = 22(33/D(\text{mm}))^{2.6} \text{ MOhms/m.} \quad (42)$$

The total transverse impedance is then $Z_T = Z_{T,h} + Z_{T,t}$. For longitudinal impedance, $Z_{L,h}/n = (D^2/8R)*Z_{T,h}$ and from W. Chou's Table 2, $Z_{L,t}/n = 0.34$ Ohms independent of liner diameter.

The instability threshold impedances given in the Collider SCDR are $Z_T = 170$ MOhms/m and $Z_L/n = 4.1$ Ohms.¹³ In the SCDR the transverse "safety margin" (the instability threshold divided by twice the calculated impedance) is 4 and the longitudinal

margin is 6. Here we need only be concerned with the transverse impedance since it has the smallest margin.

Assuming constant conductance C the dependence of $Z_{T,h}$ on hole diameter is $Z_{T,h} \sim (g/p)*(d/t)$. The factors f and g and the “normalized impedance” $(g/f)*(d/t)$ are plotted in Figures 2 and 3. Minimizing $Z_{T,h}$ with C constant leads one to choose the smallest practical hole size. This occurs in the range $d/t \sim 1-2$, below this the number of holes required and fractional surface area covered become very large. The hole thickness has been taken from our current liner designs $t = 1.25$ mm and the diameter of holes is taken as $d = 2$ mm. The Gluckstern correction factor for $t/d = 0.625$ is essentially equal to its asymptotic thick hole limit $g = 0.562$. The impedance is reduced by a factor of almost two compared to an infinitesimally thin hole.

The impedance safety margin S is defined to equal the instability threshold impedance divided by twice the calculated impedance. For a given safety margin $S = 1, 2, 3$ and 4 the relationships between the number of holes per meter and liner diameter are plotted in Figure 4. The allowable safety margin is a strong function of the liner diameter. For a safety margin of 2.0 the minimum allowed liner diameter is 25.6 mm with no allowance left for holes, for a safety margin of 1.0 the minimum liner diameter is 19.6 mm. For most of the calculations reported here a minimum safety margin of 2.0 is regarded as acceptable and the liner diameter has been chosen to be 30.2 mm. The corresponding maximum number of 2-mm holes per meter is then $N_h = 1546$. For a liner temperature $T = 80$ K the maximum conductance for H_2 is then $C_{12} = 690$ l/m/s. The transverse impedance for constant H_2 conductance $C_{12} = 690$ l/m/s is plotted in Figure 5 as a function of the diameter of liner holes for assumed liner diameters of 20.2, 25.2 and 30.2 mm. The instability threshold ($S = 0.5$) boundary is indicated by the horizontal dashed line.

The equations describing the liner vacuum have assumed that a negligible fraction of molecules exiting the liner holes hit the bore tube and scatter directly back through the holes.

For this to be true the gap between the liner and bore tube must not be too small. Assuming a $\cos(\theta)$ distribution for the backscattered molecules, upper and lower bounds for the backscatter fraction are:

$$f_U = 1 - r/(r^2 + (d/2)^2)^{1/2} \quad (43)$$

$$f_L = 1 - (r+t)/((r+t)^2 + (d/2)^2)^{1/2}.$$

where r is the radial gap width between the outside of the liner and the bore tube, d is the hole diameter and t is the liner thickness. These fractions are plotted in Figure 6 for $d = 2$ mm and $t = 1.25$ mm. For the present radial gap width $r = 4.5$ mm the backscatter fraction is less than a few percent and the gap could be reduced to 2 mm without large effect.

4.0 INPUT DATA

4.1 Hydrogen isotherm

Before discussing numerical solutions to the equations of the previous section it is useful to examine the H_2 isotherm on the 4.2 K SS bore tube wall that is not covered by cryosorber. This is shown in Figure 7 where we have plotted the BET equation and also normalized data from Benvenuti *et al.*¹⁴ measured on SS at 4.17 K.

The BET Eq. (44) has the saturation property $y = 1$ as $x \rightarrow \infty$. In Figure 7 the normalized variables are $x = s/s_m$, $y = n_e/n_{sat}$, s is the surface density of H_2 , n_e is the equilibrium vapor density, s_m the density of one monolayer, n_{sat} the saturated vapor pressure ($n_{sat}(cm^{-3}) = 6.84 \times 10^{22} e^{-95.8/T/T}$) and $\alpha = e^{\Theta/T}$. The data of Benvenuti *et al.*, have been normalized with $s_m = 6 \times 10^{15} H_2/cm^2$ and $n_{sat} = 1.73 \times 10^{12} H_2/cm^3$. The BET Eq. (44) is plotted with $\Theta = 39.7$ K, $\alpha = e^{\Theta/T} = 1.37 \times 10^4$. The rapid rise in vapor pressure near one monolayer $x \sim 1$ is of course the reason for pursuing a liner to avoid too frequent warm ups of the Collider beam tube to remove the photodesorbed H_2 . Below $x \sim 1$ the data of Benvenuti *et al.*, in Figure 7 are dominated by thermal desorption by 80 K and 300 K radiation from

other parts of the vacuum system and the vapor pressure is higher than it would be in the absence of such radiation. However, this seems to be a reasonably accurate simulation of the situation here since the 4.2 K liner faces the 80 K bore tube.

$$x = \alpha y / [(1-y)(1 + (\alpha-1)y)] . \quad (44)$$

If we make the approximation $y \ll 1$, which should be the case at very low photon dose, the BET Eq. (44) reduces to the simpler form:

$$y = x / [\alpha(1-x) + x] . \quad (45)$$

Equation (45) accounts for the very rapid rise in vapor pressure as $x \sim 1$ is approached, eventually invalidating the approximation $y \ll 1$. It is this rapid rise in vapor pressure near one monolayer which led to the two useful approximations for solving Eqs. (1) to (5) in Section 2.2. When the magnet bore tube surface reaches equilibrium $\sigma_w S_{2w} * n_{12} \equiv N_w / \tau_w$ it ceases to pump. The cryosorber is then chosen to clamp the H_2 vapor pressure well before it reaches the saturation value. Without the cryosorber the saturation vapor pressure would be reached and equilibration through the holes in the liner would lead to the same excessive pressure problem as occurs without the liner (the density decrease due to $(T_2/T_1)^{1/2}$ would not be enough to prevent overload of the cryogenic system and quenching of the magnets).

A useful estimate of the sojourn time for H_2 on SS can be obtained by using the equilibrium isotherm. When the surface is in equilibrium we have from Eq. (4):

$$\begin{aligned} \tau_w &= N_w / \sigma_w S_{2w} n_{12} \\ &\equiv 2(a_1/a_2) * (1/\sigma_w \langle v_2 \rangle) * (s/n_{21}) \\ &\equiv 4 * (1/\sigma_w \langle v_2 \rangle) * (s_m/n_{sat}) * (x/y). \end{aligned} \quad (46)$$

where $x = s/s_m$ and $y = 2n_{21}/n_{sat}$. The sojourn time should be a function only of the surface temperature and the surface density of H_2 and not depend on whether or not the surface is

actually in equilibrium—*i.e.*, not on the vapor density or incident molecular flux that is actually present. We therefore argue that Eq. (47), which has been derived from an equilibrium situation, can also be used when the surface is not in equilibrium providing n_{21} is properly calculated—*i.e.* we use the equilibrium isotherm to calculate n_{21} for a given s rather than the n_{21} that is actually present. If $x \ll 1$, which should describe a clean surface, $x/y \equiv \alpha$ and $\tau_w \equiv 4 * (1/\sigma_w \langle v_2 \rangle) * (s_m/n_{sat}) * (\alpha) = 4.3$ hrs.

For the first approximation—that the surface be far from equilibrium—we should also have the time since the start of photodesorption short compared to the sojourn time. For the second approximation—that the surface be in equilibrium—the time should be long compared to the sojourn time.

4.2 Vapor pressure of CH₄, CO and CO₂

Other gases besides H₂ are commonly observed in photodesorption experiments, the most important ones are CH₄, CO and CO₂. If the volume density of these molecules exceeds the isotherm saturation density then thick layers of these gases will build up by cryosorption. The saturation vapor density may be looked up in standard references. For example using the information in Barron¹⁵ we obtain the following saturation densities at 80 K; 2.3×10^{18} CH₄/cm³, 7.5×10^{19} CO/cm³ and 2.2×10^{10} CO₂/cm³. Generally these saturation densities exceed the expected gas densities inside the liner by a large margin so significant surface concentrations will not build up on the liner. At 4.2 K however the saturation vapor density of these molecules is vanishingly small so they will accumulate on the SS bore tube until it is warmed up.

4.3 Photodesorption data from the central design group experiment of Bintinger *et al.*^{16,17}

At the time the design study described in this report was initiated photodesorption data in a 4.2 K electroplated Cu tube was limited to the single experiment done by a SSC Central Design Group team. This experiment is described in two reports.^{16,17} Numerical values for the parameters appearing in the model equations in paragraph 2 can be extracted from these reports. The results for the photodesorption coefficients η are given in Table 1 for each of the gases measured. Desorption coefficients for CH₄ were not reported. These coefficients were measured in a beam tube at 294 K, however the experimenters concluded that for H₂ η is about the same at 4.2 K and 294 K. The basis for this conclusion is three repetitions of a photodesorption experiment done at 4.2 K and 294 K with small samples cut out of the beam tube.¹⁷ A limitation of the data from these experiments is that the maximum total integrated photon flux was 1×10^{21} photons/m which corresponds to only one day of SSC operation at design current. To obtain predictions beyond this flux it is necessary to extrapolate the data, which we have done assuming no change in the rate of decrease of η with accumulated photon flux. The motivation for this assumption is the 294 K data of Foerster *et al.*¹⁸ on various materials which are reasonably well fit with single power law decreases of η with photon flux up to 10^{23} photons/m. Furthermore this is most probably a conservative assumption since the rate of decrease with photon flux is lower than has usually been observed by other experimenters with different materials.^{18,19} For the coefficients listed in Table 1 the inverse power law dependence of photon flux is approximately 0.3.

The data from the CDG experiment differ in some details from what will occur in the Collider. The critical energy for the CDG experiment was 478 eV and the angle of incidence was 9 mrad compared to 284 eV and 2 mrad for the Collider. The data of Gomez-Goni²⁰ *et al.*, on OFHC Cu show the desorption coefficients increasing linearly with energy up to

280 eV and then increasing about a factor of 2 up to 3 keV. The angular dependence of photodesorption coefficient hasn't been measured down to 2 mrad. However the data of Grobner *et al.*²¹ indicate that at 3 keV critical energy the desorption coefficient is rather slowly increasing with decreasing angle of incidence at 11 mrad. As a result of these observations the data of the CDG experiment are used without correction for angle of incidence and critical energy. Additional details concerning the cutoff of low energy photons and different fractions of the wall circumference illuminated by the primary photon flux are also left uncorrected.

The other parameters of interest are the sticking coefficient, mean molecular speed and recycling coefficient η' . These can be estimated from the data in Ref. 16, 17 taken at 4.2 K. The results for H₂ are $\sigma_w = 1/13$, $\langle v \rangle = 1.8 \times 10^5$ cm/sec and $\eta' = 1.2$ at $\Gamma = 8.0 \times 10^{20}$ photons/m. Recycling is apparently quite large and efficient compared to primary desorption, having reached a value of approximately one molecule per photon at the conclusion of the experimental run when the direct term has fallen to less than one molecule per two hundred photons. If η' is parametrized as $\eta' = \eta'_0(s/s_m)$ then $\eta'_0 = 1.4$, where we have used $\eta_{4 K} = \eta_{294 K}$ to calculate $s = 5.1 \times 10^{15}$ H₂/cm² at $\Gamma = 8 \times 10^{20}$ photons/m and $s_m = 6 \times 10^{15}$ H₂/cm².

One year of SSC operation is projected to be 2×10^7 sec, or 2×10^{23} photons/m at design intensity. The desorption coefficients listed in Table 1, admittedly extrapolated to a total flux one hundred times larger than the maximum measured flux, can be used to estimate the amount of gas desorbed in one operational year. The results are listed in Table 2 below together with intermediate values at photon fluxes of 10^{21} , 10^{22} and 10^{23} photons/m. The total amount of H₂ desorbed at 2×10^{23} photons/m is 2.5×10^{20} H₂/m, corresponding to 44 monolayers assuming a tube diameter of 30.2 mm and a monolayer density $s_m = 6 \times 10^{15}$ H₂/m. Clearly this would require an excessive number of beam tube warm ups per year of operation if a liner or distributed pump is not present. The total amount of all

gases desorbed in one year is projected to be ~ 10 Torr l/m at 273 K. The cryosorber capacity of the distributed pump concept indicated in Figure 1 should be chosen in this range.

4.4 Scattering cross section, pumping speed ratios and relative weights of gas species in the inverse luminosity lifetime

The luminosity lifetime of a Collider proton beam due to nuclear scattering is

$$1/\tau_L = 2 * \sum_j n_j \sigma_{jp} c \quad (47)$$

where the sum is over all molecular gas species j and σ_{jp} is the total scattering cross section of a 20 TeV proton with molecule j . From Eqs. (6) and (16), in a 80 K liner configuration the density n_j is proportional to the product of the desorption coefficient η_j and the square root of the mass m_j . It is of interest to calculate the weights of the heavier gases CH₄, CO and CO₂ relative to H₂ in $1/\tau_L$ due to the different desorption coefficients, cross sections and molecular weights. The total nuclear cross section for a 20 TeV proton hitting a stationary proton is taken as $\sigma_{pp} = 50$ mb. The cross section of a 20-TeV proton hitting an atom with atomic number A is assumed to be geometric so $\sigma = A^{2/3} \sigma_{pp}$, the molecular cross section is summed over the atoms. In Table 3 we list the weights relative to H₂ in the inverse luminosity lifetime due to desorption coefficient, scattering cross section and pumping speed. The product of all three weights is also given. Although the desorption coefficients of the heavier molecules are less than for H₂, the higher cross sections and molecular weights more than compensate. The result is that for the data of Bintinger *et al.*¹⁶ the luminosity lifetime due to nuclear scattering on H₂ is reduced by a factor of ~ 12.3 when all gases are included.

5.0 NUMERICAL SOLUTIONS

5.1 4.2 K beam tube without a liner

In this section we present the prediction of H₂ build-up in a 4.2 K beam tube under Collider conditions and without a liner. The parameters of Section 4.3 deduced from Ref. 16 are used as input. A beam tube ID of 30.2 mm is assumed. H₂ density is plotted versus time in Figure 8a assuming a photon flux at design intensity 10¹⁶ photons/m/sec. The three components of the H₂ density are shown due to primary desorption, recycling and the isotherm. The isotherm density rises rapidly after 10⁵ sec or about one day of operation as the surface density of H₂ approaches one monolayer and this would prevent further operation until the beam tube is warmed up and pumped out. This rapid rise was not observed in the photodesorption experiments. There are at least three possible explanations. One is that the experiments fell somewhat short of desorbing a monolayer and the isotherm pressure was still negligible. The condition $\eta_{4K} = \eta_{294K}$ is consistent with this explanation. The second possibility is that the desorption coefficient at 4.2 K is actually less than at 294 K. The third possibility is that some molecules are lost by axial diffusion so the build up of H₂ is reduced. Returning to Figure 8a, before a monolayer is reached the dominant density component is seen to be due to recycling except at very early times. Just before a monolayer has been reached the luminosity lifetime due to scattering on H₂ alone has fallen to ~11.25 hrs. Scattering by heavier gases hasn't been included. A luminosity lifetime this low would soon require a beam tube warm up and pump out even if the rapid rise in isotherm density didn't occur.

Since the results in Figure 8a predict an initial monolayer is reached in only one day's photon flux it is of interest to have an idea how long the second, third and following monolayers will take to form. For a simple power law dependence of desorption coefficient on photon flux $\eta = \eta_0 / (\Gamma / \Gamma_0)^\alpha$ the time T_n to form the n-th monolayer is given by:

$$T_n = T_1 [n^{1/(1-\alpha)} - (n-1)^{1/(1-\alpha)}] , \quad (48)$$

and for $n \gg 1$,

$$T_n \approx (T_1/(1-\alpha)) * n^{\alpha/(1-\alpha)},$$

where

$$T_1^{1-\alpha} = (1-\alpha) A_w s_m / (\eta_0 \Gamma_0^\alpha d\Gamma/dt^{1-\alpha}).$$

The monolayer time is plotted versus monolayer number in Figure 8b for the H_2 desorption coefficient extrapolated from the experiment of Bintinger *et al.*⁴ ($\eta_0 = 0.017$, $\Gamma_0 = 10^{19}$ photons/m, $\alpha = 0.3$, $T_1 = 9.1 \times 10^4$ sec) and for baseline photon flux 10^{16} photons/m/s in the Collider. The monolayer formation time is predicted to be a rather slowly increasing function of monolayer number, behaving as the 0.43 power of the monolayer number n for $n \gg 1$ and reaching only about 5 days for $n = 20$. Beam tube warm up, pump out cycles with this frequency would place a large burden on Collider operation.

5.2 80 K liner configuration

In order to obtain numerical results we need to assume specific values for liner hole conductance and cryosorber pumping speed in addition to the molecular desorption coefficients. For the desorption coefficients we take the values give in Table 1. Ideally the pumping speed of the cryosorber should be large compared to the conductance of the liner holes. The conductance of the holes are then the limiting factor determining molecular density inside the liner. We also need to choose the hole conductance large enough so the density of H_2 falls below that required to achieve the beam lifetime goal with reasonably short conditioning of the beam tube and consistent with beam instability impedance constraints. It will turn out that the nuclear scattering lifetime of the beam is dominated by the heavier gases

CO and CO₂ however here we give the estimated requirement for H₂ alone. The goal for τ_L is 150 hrs which requires $n(H_2) < 3 \times 10^8/cm^3$. From Eq. (16) an estimate of C_{12} is:

$$C_{12} \equiv \eta * d\Gamma/dt/n(H_2). \quad (49)$$

For the H₂ desorption coefficient we take a representative initial value for electrodeposited Cu $\eta = 0.02$, choose the Collider baseline value for photon flux $d\Gamma/dt = 10^{16}$ photons/m/s and obtain $C_{12} \equiv 667$ l/m/s for H₂ at 80 K as an estimate of the region of interest. This is very close to the upper bound allowed by impedance considerations. The numerical examples in Table 4 have been calculated for the cryosorber pumping speed equal to five and two times the hole conductance and for hole diameters 1, 2 and 3 mm. The molecular transmission probability p of the holes is tabulated assuming a hole thickness 1.25 mm. For all the cases given in Table 4 the reciprocal combination of C_{12} and S_c has been held constant at 460 l/m/s H₂ at 80 K.

The final choice of hole size and shape and the pattern of the holes will depend on considerations of the RF impedance and cost. It isn't known yet what value of S_c can be achieved in a liner configuration with the cryosorber facing the 80 K surface. To get some idea of what is practical we calculate the fraction of the bore tube surface that must be covered with cryosorber in order to obtain the pumping speeds $S_c = 1380$ and 2760 l/m/s. The fractions are $0.045/\sigma\omega$ and $0.09/\sigma\omega$, respectively, where $\sigma\omega$ is the sticking coefficient. For a sticking coefficient near unity there is no problem. A sticking coefficient as low as 0.1 would give difficulty. Although the net pumping speed for all the cases listed in Table 4 is equivalent to an ideal pump with 2.1% of the liner area (assuming a liner ID = 30.2 mm), the actual fraction of the liner surface area perforated with holes is 5.5%, 4.1% and 3.6% for the $C_{12} = 552$ l/m/s cases in Table 2 and 6.9%, 5.1% and 4.5% for $C_{12} = 690$ l/m/s.

Calculations for the 80 K liner case are shown in Figures 9 to 12. For these calculations we have assumed the liner ID = 30.2 mm, the liner conductance is specified by $N_h = 1546$

2 mm diameter, 1.25 mm thick holes/m and the cryosorber H₂ pumping speed is $S_c = 1380 \text{ l/m/s}$. H₂ densities inside and outside the liner are shown in Figures 9a and 9b, the surface density of H₂ building up on the 4.2 K bore tube is given in Figure 10. The H₂ density shown in Figure 9b is actually a normalized density $2n_{21}/n_{\text{sat}}$ where n_{sat} is the H₂ saturation isotherm density at 4.2 K. In our two component model of the gas between the 80 K liner and 4.2 K bore tube this normalized density would approach unity in the absence of cryosorber and as the surface density of H₂ builds up to a monolayer on the bore tube. The actual density of H₂ in this region is $n_{21} + n_{12} = (1 + (T_2/T_1))^{1/2}n_{21} = 1.23*n_{21}$. The solutions are shown for the two approximations given by Eqs. (6) to (10) and (11) to (15) above, before and after the surface of the magnet bore tube reaches equilibrium. The transition from the first to the second approximation occurs when the two solutions for the surface density of H₂ on the bore tube are equal, or from Figure 10 at a photon flux $\sim 8 \times 10^{20} \text{ photons/m}$. Near the transition the surface density of H₂ on the bore tube is approaching a monolayer—actually reaching $s/s_m = 0.65$ in Figure 10—and the isotherm density is rising rapidly until it reaches a value limited by the cryosorber pumping speed. When this happens the SS bore tube effectively ceases to pump H₂ and all the net pumping is by the cryosorber. This causes an upward jump in H₂ density inside and outside the liner at $\Gamma = 8 \times 10^{20} \text{ photons/m}$ as evidenced in Figure 9a and 9b. In Figure 9b the density jump outside is to about 10^{-4} times the H₂ isotherm saturation density. Without the cryosorber the density $2n_{21}$ would have increased to the saturation density $2 \times 10^{12} \text{ H}_2/\text{cm}^3$ outside the liner and $(T_2/T_1)^{1/2} \times 2 \times 10^{12} = 4.6 \times 10^{11} \text{ H}_2/\text{cm}^3$ inside. When the cryosorber begins to saturate (not shown in Figures 9 to 12) the H₂ density will increase toward this level which of course would require warming up the beam tube and removing the H₂. The capacity of the cryosorber must be chosen so this occurs only infrequently, estimates of the capacity required for one warm up per year are given in the right hand column of Table 2. What one gets with the liner is a photon shield for the cryosorbed molecules and an increase in the

effective surface area of the bore tube. For the desorption coefficients given in Table 1 the desired increase in effective surface area is in the range of 50 to 100.

The density of H_2 inside the beam tube is less than $3 \times 10^8/cm^3$ even at 10^{19} photons/m and decreasing with increasing photon flux. The liner/cryosorber effectively solves the H_2 isotherm problem so we next look at the effect of heavier molecules. The isotherm densities of these molecules at 4.2 K are negligibly low so the 4.2 K magnet bore tube will always remain an effective pump for them. The densities of these molecules are given by Eqs. (6) to (10) with appropriate substitutions of the desorption coefficients from Table 1 and the mass dependence of conductances and pumping speeds. The densities of CO and CO_2 inside the liner are given in Figure 11. For the desorption coefficients that have been chosen the CO density is actually comparable in magnitude to H_2 . The beam lifetime estimates for nuclear scattering on H_2 only and on H_2 , CO and CO_2 are given in Figure 12. At 10^{19} photons/m the beam lifetime is reduced from 380 hrs for H_2 only to 30 hrs with CO and CO_2 included. However the liner surface is cleaning up with increased exposure. By 1.5×10^{22} photons/m, or ~ 17 days of Collider operation at design intensity, the beam lifetime has reached the vacuum design goal of 300 hrs. If such a vacuum system were actually implemented it is likely that this vacuum conditioning would occur over a longer period of time during initial Collider operation at 20 TeV but at beam current less than the design goal. Since the synchrotron radiation intensity is proportional to beam current, the molecular densities and inverse scattering lifetime are also proportional to beam current.

6.0 WORK IN PROGRESS

When this study was begun parallel efforts were initiated to increase the photodesorption data base relevant to the SSCL Collider. The thrust of these efforts is threefold; (1) to obtain photodesorption coefficients with total photon exposures equivalent to one year of Collider operation, (2) to revive photodesorption experiments at 4.2 K and (3) to expand the list of

beam tube materials and preparation procedures under consideration. Most of the work in these areas still remains to be done; however, some new results are available and will be briefly described here.

Photodesorption coefficients for samples from the same batch of electrodeposited Cu tubing used in Refs. 16, 17 have recently been measured at 294 K up to 2×10^{22} photons/m at the Budker Institute of Nuclear Physics (BINP) VEPP-2M electron/positron collider and up to 2×10^{23} photons/m at the BNL NSLS UV ring.²² In addition Mathewson *et al.* at CERN have been taking low intensity data on the EPA machine for the LHC.²⁰ Although most of CERN work is at the LHC critical energy 64 eV, some data is taken at the SSCL Collider critical energy 284 eV and this has been useful for comparing to the work at BINP and BNL. The desorption coefficients from the experiments at BINP and BNL are given in Table 5. The two data sets agree within a factor of two except for CO₂ which has somewhat larger photodesorption coefficient for the BNL data. For photon flux within the measurement range of the experiment in Ref. 16 (*i.e.*, less than 10^{21} photons/m) they are in reasonable agreement with that experiment as well. However for photon fluxes exceeding 10^{21} photons/m the photodesorption coefficients of the new data decrease more rapidly with increasing photon flux than extrapolation from Ref. 16 suggests. The amount of H₂ desorbed by one operating year of photon flux 2×10^{23} photons/m is 4.5×10^{19} H₂/m for the BNL data and 7.4×10^{19} H₂/m for the extrapolated BINP data.²² This is significantly less than the 2.5×10^{20} H₂/m projected in Table 2 but still large enough that a liner would be an operational benefit. Anashin *et al.*²³ have used the isotherm method to measure the monolayer density of H₂ on the electroplated Cu used in these experiments, obtaining $s_m \equiv 3 \times 10^{15}$ H₂/cm². The number of equivalent monolayers desorbed in one year is then in the range 16 to 26.

The coefficients in Table 5 can be used as input to the liner calculations done in paragraph 5 and the operation time until the beam lifetime due to vacuum exceeds 300 hrs

can be estimated. The result is that the clean up time for the 80 K liner is 1 to 3 days instead of 17 days. An obvious thing to do at this point is decrease the number of holes in the liner, thus increasing the impedance instability margin at the expense of some increase in clean up time. Another possibility is to keep the number of holes fixed and calculate the liner clean up times for lower liner temperatures –0 20 K and 4.2 K. These clean up times are given in Table 6 below for the extrapolated scaling obtained from Ref. 16 and for the recent BNL and BINP data. The clean up time becomes progressively longer as the temperature is decreased because of the decreasing hole conductance in Eqs. (6), (11), (30) and (37). The molecular velocity has been assumed to equal that of a molecule in thermal equilibrium with the wall. We see from the Table 6 that with the new data even the 4.2 K liner has an acceptable clean up time, in the range of 15 days, and that this conclusion does not depend on extrapolation of data beyond its measurement range. This is in contrast to the earlier calculations which gave a clean up time of 174 days for a 20 K liner and much longer for a 4.2 K liner. Because of these unfavorable clean up times and the desire to maintain an impedance margin of at least 2.0 we had originally selected 80 K for the liner temperature. The consequence of the new data is that more possibilities are opened up, each with their own advantages. The 20 K and 80 K options would have about equal engineering complexity since they both require GHe cooling tubes. The problem of heat leaks to the 4.2 K system due to thermal radiation and thermal conduction through supports is reduced for 20 K compared to 80 K. However the refrigeration capacity available in the Collider is much larger at 80 K (650 kW) than 20 K (150 kW) and the thermal efficiency is improved at 80 K. If sufficiently good thermal contact between the “4.2 K” liner and magnet bore tube can be made so that the GHe cooling tubes can be eliminated then the 4.2 K case is less complex than 80 K/20 K. Furthermore cryosorber could be applied to the outside of a 4.2 K liner rather than the inside of the bore tube and this would also be simpler. In this case it isn’t necessary that the liner temperature be held right at the bore tube temperature, but the

temperature should be low enough that the cryosorber performs adequately. The disadvantage of a 4.2 K liner compared to 80 K/20 K is that the beam operating current is tied to the 4.2 K refrigeration capacity (67.5 kW). A factor three increase in beam current would require 36 kW additional 4.2 K refrigeration due to the increase in synchrotron radiation.

In addition to the new 294 K results the first 4.2 K photodesorption experiment at BINP has been completed with electrodeposited Cu.²³ These results and follow-on experiments will eventually have even more impact on the Collider beam tube vacuum design. It is too early to include an analysis based on these results in this report but some comments may be made. As observed in Ref. 16 the density in the 4.2 K tube, at least initially, increases with photon dose. At an integrated photon flux 8×10^{20} photons/m the magnitude of H₂ density rise observed in these two experiments appears to agree within a factor of about two. This confirms the importance of photodesorption of cryosorbed molecules. In contrast to Ref. 16 however the 4.2 K desorption coefficients are somewhat lower than at 294 K. More analysis and data at higher photon dose are needed to understand the full implications for the Collider. The results however are in the direction of decreasing the required pumping speed and therefore the number of holes and/or the temperature of the liner. For the electrodeposited Cu that has been tested it still seems that there would be a large operational benefit if a liner is installed.

Whether or not a beam tube material or preparation procedure can be found in a reasonable time frame that eliminates the vacuum need for a liner or distributed pump isn't yet known. A number of approaches are being investigated and much more information will be available in the coming year. The emphasis up to now has been on getting hardware in place so that evaluations can be made.

7.0 SUMMARY

Model equations have been developed for describing liner configurations of the SSCL Collider beam tube vacuum system that deal with the photodesorption of gases by synchrotron radiation in a superconducting magnet environment. The liner is an effective solution to the problems of desorption of cryosorbed gas and the H₂ isotherm which occur in a 4.2 K beam tube without a liner. Generally the prediction of vacuum performance depends on far fewer parameters with a liner than without. With conservative assumptions this makes it possible to specify a liner that will simultaneously meet design goals for accelerator availability and impedance constraints. Most of the calculations in the paper have dealt with an 80 K liner. Whereas a 4.2 K beam tube without a liner needs to be periodically warmed up to remove cryosorbed gases, a liner needs a certain amount of conditioning time before the beam lifetime goal can be reached. A particular example given in the report, with beam instability safety margin 2.0, indicated that an 80 K liner would need about two weeks of operating time at design intensity to reach the beam lifetime goal of 150 hrs. The 4.2 K beam tube without liner allowed only a few days of operation before it would need to be warmed up.

New photodesorption data have become available which indicate the photodesorption coefficients are somewhat less than the values used when this work was begun. It is still an open question and under vigorous research whether a beam tube material or conditioning method can be found which will allow sufficient Collider availability without a liner or distributed pump. The new photodesorption data at 294 K allow consideration of 4.2 K and 20 K liners that meet impedance budget constraints and also have adequately short conditioning times. Furthermore recent 4.2 K and 77 K photodesorption experiments at BINP indicate that the desorption coefficients decrease with temperature so the impedance of a liner, if needed, can be reduced and still have short conditioning time. Ultimately the 4.2 K experiments should be able to resolve the question of whether a liner is needed for a given beam tube material and, if needed, to define the minimum liner conductance.

REFERENCES

¹H. Edwards, "Study on Beam Tube Vacuum with Consideration of Synchrotron Light, Potential Liner Intercept, and Collider Quad/Spool Coil Diameter," SSCL-N-771. August (1991).

²LHC Study Group, "Design Study of the Large Hadron Collider (LHC)," CERN 91-03 (1991).

³Q.-S. Shu *et al.*, "Prototype Liner System for the Interception of Synchrotron Radiation in a Half Cell for the SSCL Collider," Proc. of the IEEE Particle Accelerator Conference, Washington, D.C., May 17–20, 1993.

⁴H. Edwards, "Study on Beam Tube Vacuum with Consideration of Synchrotron Light, Potential Liner Intercept, and Collider Quad/Spool Coil Diameter," SSCL-N-771. August (1991) and A. Maschke, "Hydrogen Desorption and the Search for the Higgs," SSCL-Preprint 86. March (1992).

⁵SSC Central Design Group, "Conceptual Design of the Superconducting Super Collider," SSC-R-2020. March (1986).

⁶R. Carcagno, W. Schieller, H.-J. Shih, X. Xu and A. Yucel, *Proceedings of Supercollider IV*, New Orleans (1992).

⁷S. Brunauer, P. Emmett, and E. Teller, J. Chem. Soc. **60**, 309 (1938).

⁸S. Kurennoy, Particle Accelerators **39**, 1 (1992).

⁹R. Gluckstern, "Coupling Impedance of a Single Hole in a Thick Wall Beam Pipe," and "Coupling Impedance of Many Holes in a Liner Within a Beam Pipe," Phys. Rev. A **46**, 1106, **46**, 1110 (1992).

¹⁰E. Ruiz, L. Walling, Y. Goren, and N. Spayd, report in preparation.

¹¹W. Chou and T. Barts, report in preparation.

¹²J. O'Hanlon, *A User's Guide to Vacuum Technology* (J. Wiley, New York 1989).

¹³J. Sanford and D. Mathews, eds., "Site-Specific Conceptual Design of the Superconducting Super Collider," SSCL-SR-1056. July (1990).

¹⁴C. Benvenuti, R. Calder, and G. Passardi, *J. Vac. Sci. Technol.* **13**, 1172 (1976).

¹⁵R. Barron, *Cryogenic Systems*, 2nd edition (Oxford Univ. Press, 1985).

¹⁶D. Bintinger, P. Limon, H. Jostlein, and D. Trbjovic, "Status of the SSC Photodesorption Experiment," SSC-102 (1986).

¹⁷D. Bintinger, P. Limon, and R. Rosenberg, *J. Vac. Sci. Technol.* **A7**, 59 (1989).

¹⁸C. Foerster, H. Halama, and C. Lanni, *J. Vac. Sci. Technol.* **A8**, 2856 (1990).

¹⁹A. Mathewson, private communication.

²⁰J. Gomez-Goni, O. Grobner, and A. Mathewson, CERN, CH-1211 Geneve 23, Switzerland, *Vac. Tech. Note* 92-12 (1992).

²¹O. Grobner, A. Mathewson, H. Stori, R. Strubin, and R. Souchet, *Vacuum* **33**, 397 (1983).

²²I. Maslennikov *et al.*, "Photodesorption Experiments on SSC Collider Beam Tube Configurations," SSCL-Preprint-378. To appear in *Proc. of the IEEE Particle Accelerator Conference*, Washington, D.C., May 17-20, 1993.

²³V. Anashin, V. Evtigneev, O. Malyshev, V. Osipov, I. Maslennikov, and W. Turner, "Summary of Recent Photodesorption Experiments at VEPP2M," SSCL-N-825 (June, 1993).

TABLES

TABLE I. Photodesorption coefficients versus photon dose from Ref. 16 for 294 K electroplated Cu molecules/photon.

Gases	Molecules/Photon				
	10^{19} photons/m	10^{20}	10^{21}	10^{22*}	10^{23*}
H ₂	2.5×10^{-2}	8.5×10^{-3}	4.3×10^{-3}	2.1×10^{-3}	1.1×10^{-3}
CH ₄	—	—	—	—	—
CO	9.0×10^{-3}	3.0×10^{-3}	1.4×10^{-3}	6.8×10^{-4}	3.3×10^{-4}
CO ₂	2.6×10^{-3}	9.0×10^{-4}	4.2×10^{-4}	2.0×10^{-4}	9.3×10^{-5}

*all desorption coefficients above 10^{21} photons/m are extrapolated

TABLE II. Quantity of desorbed gas verses photon dose estimated from extrapolation of the data of Ref. 16.

Gases	Molecules/m (Torr l/m*)			
	10^{21}	10^{22*}	10^{23*}	$2 \times 10^{23*}$
	photons/m			(one oper yr)
H ₂	6.1×10^{18}	3.0×10^{19}	1.6×10^{20}	2.5×10^{20} (7.1**)
CH ₄	-	-	-	-
CO	2.1×10^{18}	1.0×10^{19}	4.8×10^{19}	7.7×10^{19} (2.2**)
CO ₂	6.3×10^{17}	3.0×10^{18}	1.4×10^{19}	2.2×10^{19} (0.6**)

* Quantities of desorbed gas above 10^{21} photons/m are extrapolated

** Torr l/m at 273 K

TABLE III. Inverse luminosity lifetime weights of CH₄, CO and CO₂ relative to H₂.

Gases	w _η *	w _m	w _σ	w
H ₂	1	1	1	1
CH ₄	—	2.8	4.6	—
CO	0.33	3.7	5.8	7.1
CO ₂	0.10	4.7	9.0	4.2
TOTAL				12.3

* from column 4 Table I

TABLE IV. Density of 80 K liner holes.

d (mm)	p	N _h (holes/m)	
		C ₁₂ =552 l/m/s*	C ₁₂ =690 l/m/s*
		Sc=2760 l/m/s*	Sc=1380 l/m/s*
1	0.46	6668	8335
2	0.62	1237	1546
3	0.71	480	600

*for H₂ at 80 K

TABLE V. 294 K photodesorption coefficients from recent experiments.

(a) Photodesorption coefficients versus photon dose measured at BINP for 294 K electroplated Cu (Ref. 22)

Gases	Molecules/Photon				
	10^{19}	10^{20}	10^{21}	10^{22}	10^{23*}
photons/m					
H ₂	3.4×10^{-2}	1.5×10^{-2}	3.7×10^{-3}	9.4×10^{-4}	2.4×10^{-4}
CH ₄	6.8×10^{-4}	2.9×10^{-4}	7.3×10^{-5}	1.8×10^{-5}	4.5×10^{-6}
CO	5.7×10^{-3}	2.5×10^{-3}	6.2×10^{-4}	1.6×10^{-4}	3.9×10^{-5}
CO ₂	1.2×10^{-3}	5.2×10^{-4}	1.3×10^{-4}	3.3×10^{-5}	8.2×10^{-6}

(b) Photodesorption coefficients versus photon dose measured at BNL for 294 K electroplated Cu (Ref. 22)

Gases	Molecules/Photon				
	10^{19}	10^{20}	10^{21}	10^{22}	10^{23*}
photons/m					
H ₂	5.8×10^{-2}	1.55×10^{-2}	3.9×10^{-3}	6.6×10^{-4}	1.2×10^{-4}
CH ₄	8.5×10^{-4}	2.9×10^{-4}	6.4×10^{-5}	8.0×10^{-6}	4.9×10^{-7}
CO	1.2×10^{-2}	4.5×10^{-3}	1.0×10^{-3}	1.4×10^{-4}	9.6×10^{-6}
CO ₂	7.9×10^{-3}	3.5×10^{-3}	6.8×10^{-4}	8.5×10^{-5}	9.4×10^{-6}

*all desorption coefficients above 10^{22} photons/m are extrapolated

TABLE VI. 80 K, 20 K and 4.2 K liner clean up time (1546 2-mm holes/m).

 (a) CDG data^{16,17}

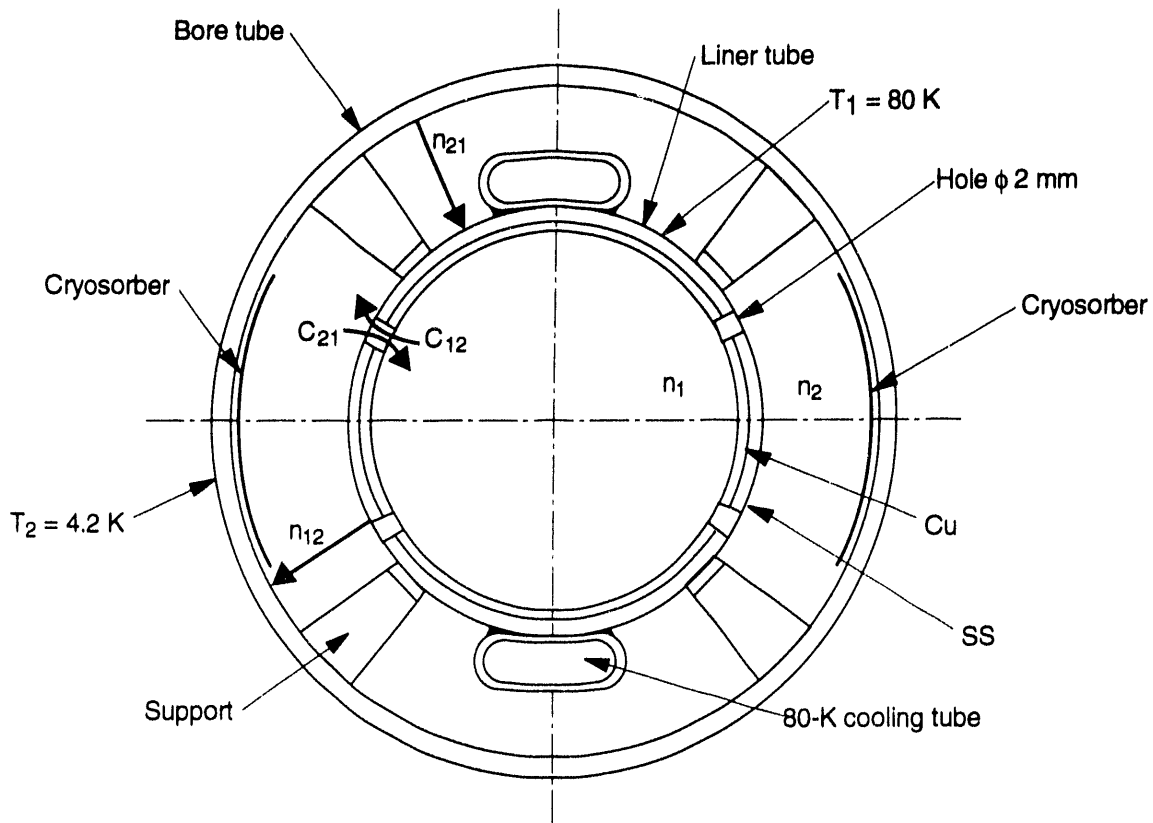
Liner temp (K)	H ₂ conductance (liters/m/s)	Photon flux to achieve t _b = 300 hrs (photons/m)	Operation time to achieve t _b = 300 hrs (days)
80	690	1.5×10 ²²	17
20	345	1.5×10 ²³	174
4.2	158	1.6×10 ²⁴	1852

 (b) BNL024²²

Liner temp (K)	H ₂ conductance (liters/m/s)	Photon flux to achieve t _b = 300 hrs (photons/m)	Operation time to achieve t _b = 300 hrs (days)
80	690	2.8×10 ²¹	3.2
20	345	6.5×10 ²¹	7.5
4.2	158	1.3×10 ²²	15.1

(c) BINP009²²

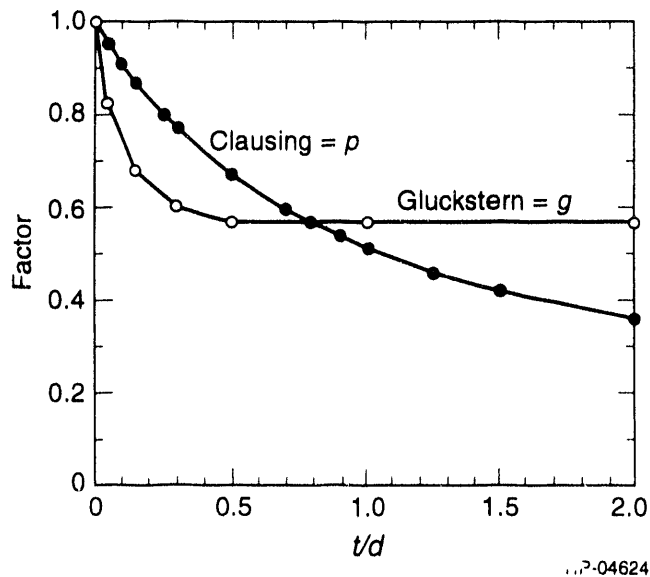
Liner temp (K)	H ₂ conductance (liters/m/s)	Photon flux to achieve t _b = 300 hrs (photons/m)	Operation time to achieve t _b = 300 hrs (days)
80	690	1.05×10 ²¹	1.2
20	345	3.5×10 ²¹	4.1
4.2	158	1.3×10 ²²	15.1



Design option of dipole liner cross section
(Total hole area/total tube area = 2.4%)

TIP-04623

FIG. 1. Liner schematic.



TIP-04624

FIG. 2. Clausing and Gluckstern correction factors versus the ratio of hole thickness versus diameter.

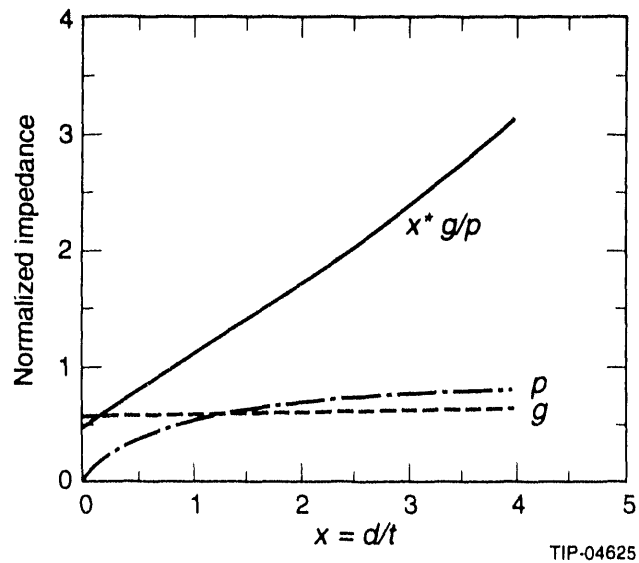


FIG. 3. Hole impedance normalized for constant conductance versus the ratio of hole diameter to thickness.

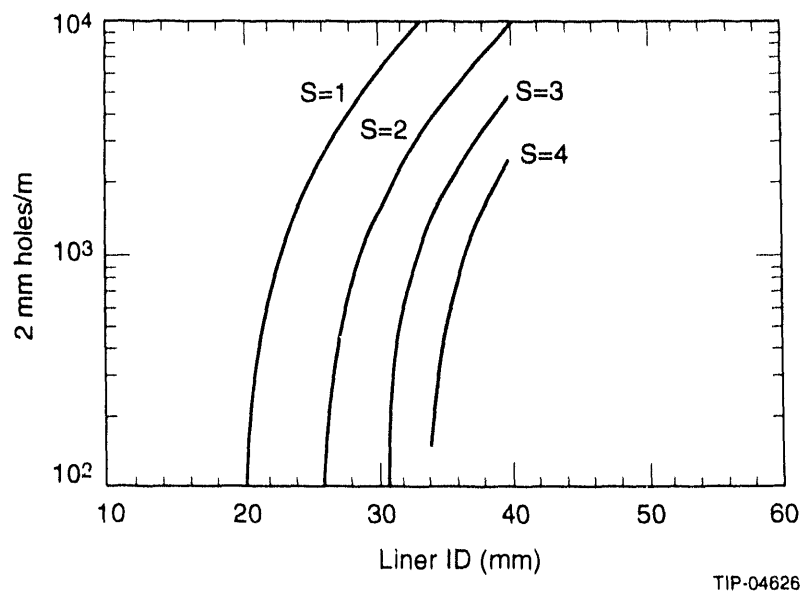


FIG. 4. Number of liner holes per meter versus liner ID for impedance safety margins $S = 1$, 2, 3, and 4, hole diameter = 2 mm, hole thickness = 1.25 mm.

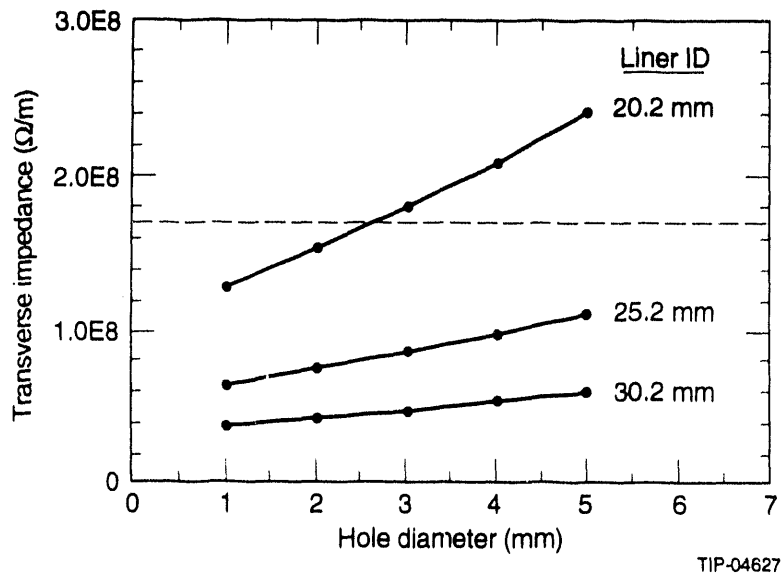


FIG. 5. Transverse impedance versus hole diameter for H_2 conductance $C_{12} = 690 \text{ l/m/s}$.

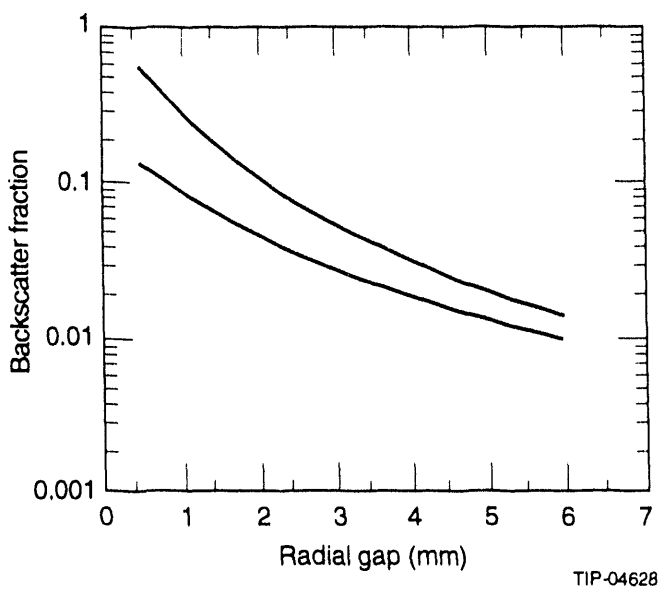


FIG. 6. Backscatter fraction versus radial gap between the liner and bore tube.

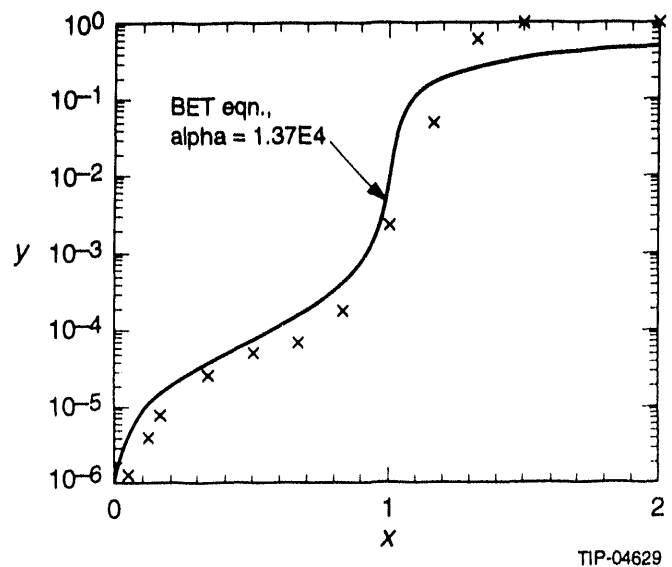


FIG. 7. H_2 isotherm on SS at 4.17 K.

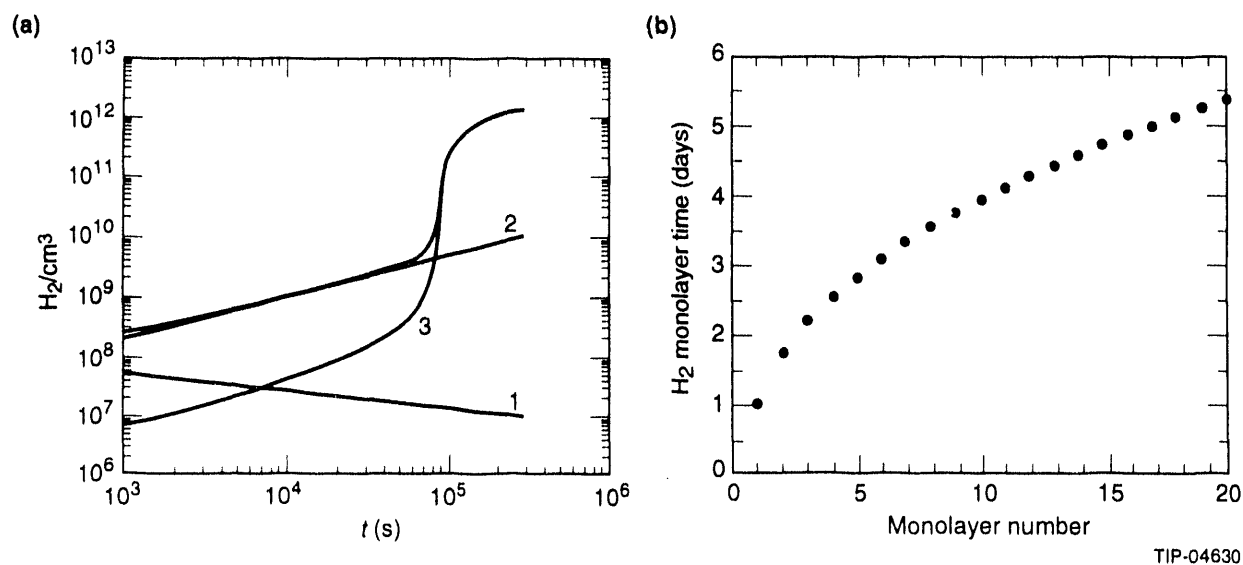


FIG. 8. (a) Predicted H_2 density vs. time for $d\Gamma/dt = 10^{16}$ photons/m/s and no liner and (b) H_2 monolayer formation time vs. cumulative number of monolayers desorbed.

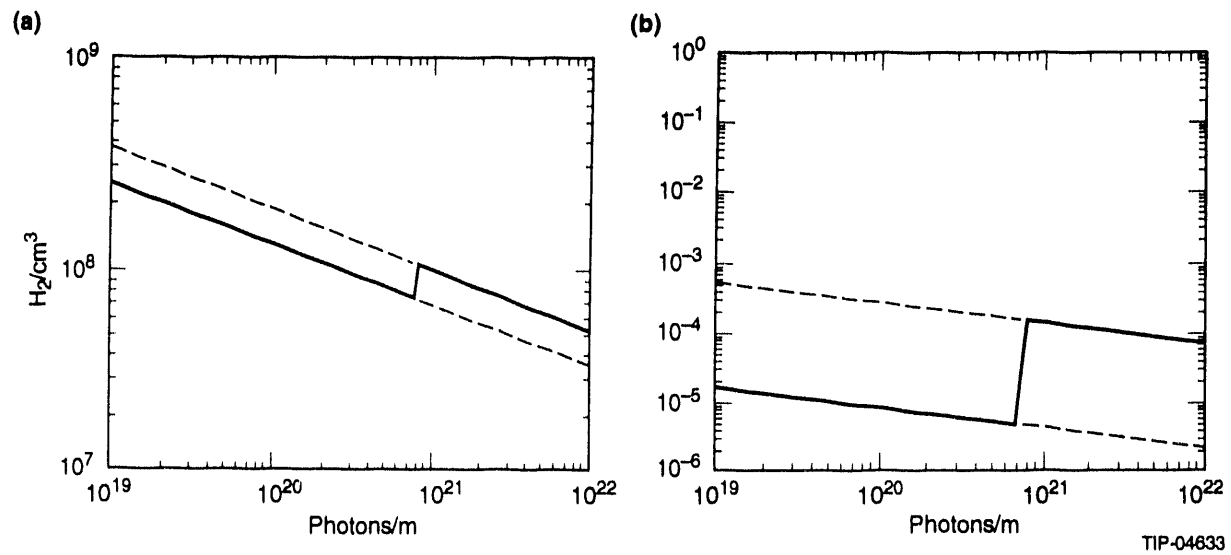


FIG. 9. (a) H₂ density inside the 80 K liner, 1 = primary desorption, 2 = recycling, 3 = isotherm; (b) Normalized H₂ density between the 80 K liner and 4.2 K magnet bore tube.

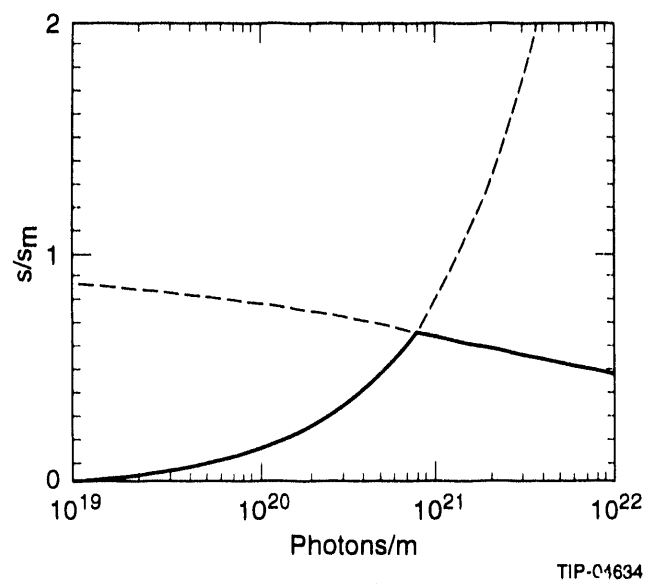


FIG. 10. Normalized surface density of H₂ on the 4.2 K magnet bore tube.

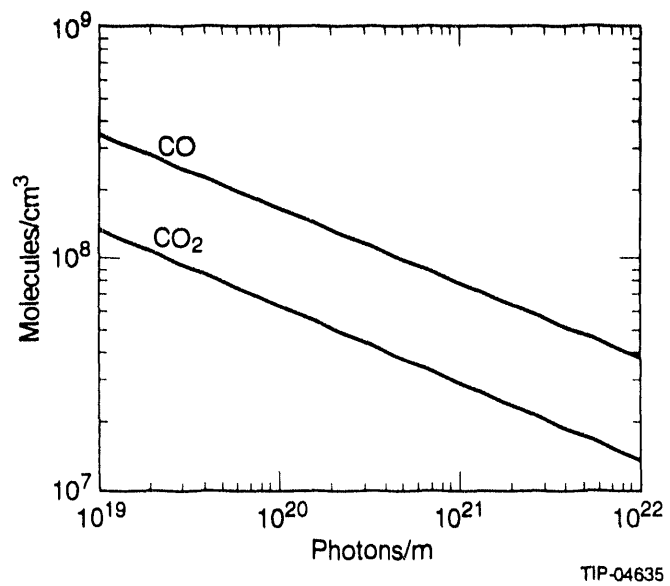


FIG. 11. Density of CO and CO₂ inside the 80 K liner.

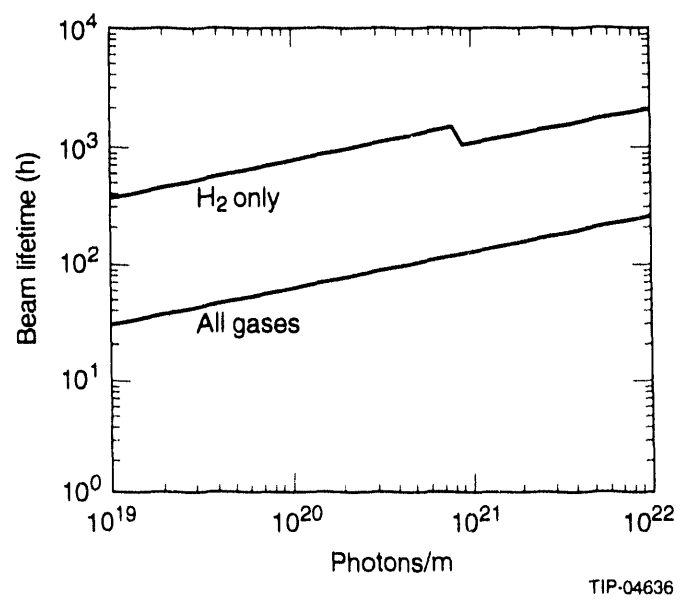


FIG. 12. 20 TeV proton nuclear scattering lifetime with an 80 K liner.

END

DATE
FILMED

12/22/93

